WILEY | Hindawi

Research Article

CO$_2$-Philic [EMIM][Tf$_2$N] Modified Silica in Mixed Matrix Membrane for High Performance CO$_2$/CH$_4$ Separation

Siti Nur Alwani Shafie,[1] **Wen Xuan Liew,**[1] **Nik Abdul Hadi Md Nordin** (iD)**,**[1]
Muhammad Roil Bilad (iD)**,**[1,2] **Norazlianie Sazali,**[3,4]
Zulfan Adi Putra,[1] **and Mohd Dzul Hakim Wirzal** (iD)[1]

[1]*Department of Chemical Engineering, Universiti Teknologi PETRONAS (UTP), 32610 Seri Iskandar, Perak Darul Ridzuan, Malaysia*
[2]*Jurusan Pendidikan Kimia, Institut Keguruan Ilmu Pendidikan, Jalan Pemuda No. 59A, Mataram, Indonesia*
[3]*Advanced Membrane Technology Research Centre (AMTEC), Universiti Teknologi Malaysia (UTM), 81310 Skudai, Johor, Malaysia*
[4]*Centre of Excellence for Advanced Research in Fluid Flow (CARIFF), Faculty of Mechanical Engineering, Universiti Malaysia Pahang, 26600 Pekan, Pahang, Malaysia*

Correspondence should be addressed to Nik Abdul Hadi Md Nordin; nahadi.sapiaa@utp.edu.my

Separation of carbon dioxide (CO$_2$) from methane (CH$_4$) using polymeric membranes is limited by trade-off between permeability and selectivity as depicted in Robeson curve. To overcome this challenge, this study develops membranes by incorporating silica particles (Si) modified with [EMIM][Tf$_2$N] ionic liquid (IL) at different IL:Si ratio to achieve desirable membrane properties and gas separation performance. Results show that the IL:Si particle has been successfully prepared, indicated by the presence of fluorine and nitrogen elements, as observed via Fourier-Transform Infrared Spectroscopy (FTIR) and X-ray Photoelectron Spectrometer (XPS). Incorporation of the modified particles into membrane has given prominent effects on morphology and polymer chain flexibility. The mixed matrix membrane (MMM) cross-section morphology turns rougher in the presence of IL:Si during fracture due to higher loadings of silica particles and IL. Furthermore, the MMM becomes more flexible with IL presence due to IL-induced plasticization, independent of IL:Si ratio. The MMM with low IL content possesses CO$_2$ permeance of 34.60 ± 0.26 GPU with CO$_2$/CH$_4$ selectivity of 85.10, which is far superior to a pure polycarbonate (PC) and PC-Sil membranes at 2 bar, which surpasses the Robeson Upper Bound. This higher CO$_2$ selectivity is due to the presences of CO$_2$-philic IL within the MMM system.

1. Introduction

Natural gas is among the favorable energy sources due to its low greenhouse gases emissions than other fossil fuels. It is commonly used as fuel for heating, vehicle fuel, and electricity generation. However, natural gas extraction is accompanied by various impurities, which largely consist of carbon dioxide (CO$_2$) gas that can reach as high as 80% [1, 2]. The presence of CO$_2$ would reduce the calorific value of the natural gas and make it corrosive to the pipelines during transportation [3]. Ineffective CO$_2$ removal also leads to increased maintenance and processing costs. Therefore, CO$_2$ concentration must be lowered below 2% to minimize the pipeline corrosion [2, 4].

There are currently conventional techniques for CO$_2$ removal such as chemical absorptions, cryogenic, and membrane separation. Due to limitations of chemical absorption and cryogenic separation (i.e., high operating cost, process complexity and energy intensive), membrane technology for CO$_2$ removal is a promising technique. It offers low operating and capital costs, ease of installation and operation, minimal energy consumption, and low footprint [5]. Separation of CO$_2$/CH$_4$ commonly uses polymeric membranes due to their ease of production compared to inorganic ones [6, 7]. Gas separation in the dense membranes occurs by a solution-diffusion mechanism which is governed by diffusion and solubility coefficients [8]. Current performance of commercial polymeric membranes for CO$_2$/CH$_4$ separation still

operates under the Robeson Upper Bound (that shows trade-off limit between permeability and selectivity) which restricts its widespread applicability [3].

In recent years, a composite between polymeric membrane and inorganic particle has been developed, commonly known as mixed matrix membrane (MMM). MMM attracts attention due to its improved separation performances and its potential to perform beyond the Robeson Upper Bound [9–13]. Bisphenol A polycarbonate (PC) has been established as one of the developing polymer material for gas separation. Koros *et al.* [14] reported on the gas transport properties of PC with CO_2 up to 8.5 barrer with CO_2/CH_4 selectivity of 25. Similarly, Hacarlioglu *et al.* [15] studied on the effect of various preparation parameters and thermal history on PC membrane performance and found CO_2 permeability up to 7 barrer with CO_2/CH_4 selectivity of 20. Later on, Hacarlioglu *et al.* [16] introduced polypyrrole as electrically conductive powder fillers incorporated into PC membrane and obtained 62 times improvement in CO_2 permeability but loss in selectivity at higher loading due to agglomeration. Silica is one of the conventional classes of inorganic fillers that has gained much attentions throughout the development of MMM. It can be categorized into nonporous and ordered mesoporous silica [17–19]. Ahn *et al.* [20] used nonporous silica filler and found that it affected the polymer chain packing in glassy and high free-volume polymers which further altered the molecular packing of the polymer chains, resulting in better MMM permeations. Xing & Ho [21] also incorporated fumed silica into a crosslinked polyvinylalkohol-polysiloxane which showed encouraging results in improving the CO_2 permeability and selectivity. In a more recent study, Chen *et al.* [22] achieved 4 times higher of CO_2 permeability using microcellular polymers incorporated with pure silica nanoparticles.

Ionic liquids (ILs) consist of ions with melting point below $100°C$ [23]. $[EMIM][TF_2N]$ (1-Ethyl-3-methylimidazolium bis(trifluoromethanesulfonyl)amide) is one of the many room temperature ionic liquids (RTILs). RTIL is a type of molten electrolyte that has many attractive properties such as nonflammability, high thermal stability, solubility in wide range of organic and inorganic compounds and also negligible vapor pressures [24]. Blending of ionic liquid onto polymeric membranes has long been studied and shown promising results in improving membrane permeabilities and selectivities [25–28]. Hao *et al.* [28] improved the CO_2 permeability and selectivity of IL-based MMM by blending $[EMIM][Tf_2N]$ with poly(RTILs) $[vBIM][Tf_2N]$ for separation of CO_2/N_2 and CO_2/CH_4. The resulting MMM posed CO_2 permeability of 200-300 barrer with 14-17 CO_2/CH_4 selectivity. IL-modified filler was also reported to improve gas permeation properties. Hudiono *et al.* [29] impregnated zeolite SAPO-34 using $[EMIM][Tf_2N]$ and incorporated it into a poly(RTIL) membrane. They reported an increase of CO_2 and CH_4 permeability by 63% and 50% respectively, with an increase of CO_2/CH_4 selectivity by 11%. Similarly, Li *et al.* [30] embedded IL onto the outer surface of zeolitic imidazole framework (ZIF-8) and resulted in an increase of CO_2 permeance by 20% and CO_2/CH_4 selectivity by 75%.

It should be noted that the previous works embedded IL onto filler through pore impregnation. Hence, it
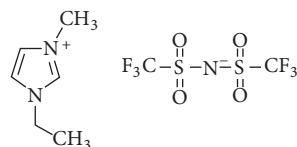

Figure 1: Molecular structure of $[EMIM][TF_2N]$.

is only applicable only when the fillers are porous. While incorporating IL onto nonporous silica has been reported as heavy metal adsorbent [31], their potential for MMM, specifically for CO_2/CH_4 separation, is yet to be evaluated. Hence, in this research, the IL-modified nonporous silica is utilized as inorganic fillers and the performances of the resulting MMM are evaluated. The silica fillers will first synthesized and modified with IL (at different ratio) before incorporated into PC membrane. The performance of the fabricated MMM will be evaluated with neat PC membrane for comparison. In authors' opinion, this is the first attempt for IL-functionalized silica incorporation into MMM. Different $[EMIM][TF_2N]$:Silica (IL:Si) ratio were prepared to comprehend the role of IL in the resulting membrane.

2. Experimental

2.1. Materials. Polycarbonate (PC) with 254.3 g/mol and density of 1.20 g/cm^3 was purchased from LG-DOW Ltd, which was then used as the polymer due to its good balance between intrinsic permeability and selectivity [32]. Dichloromethane (DCM) (Merck Ltd., boiling point of $39.6°C$) was used as solvent for membrane fabrication due to its low boiling point to induce dry inversion. 1-Ethyl-3-methylimidazolium bis(trifluoromethylsulfonyl)imide ($[EMIM][Tf_2N]$ (Figure 1), 97%) as IL was purchased from Sigma Aldrich. The silica precursor consisting of tetraethyl orthosilicate (TEOS), hydrocloric acid (HCl, 37%), and ethanol (99.5% purity) was obtained from Merck Ltd. All chemicals were used without further purification.

2.2. Silica Particle Synthesis. The silica particle synthesis procedure was adapted from Buckley & Greenblatt (1994) [33]. The sol-gel was prepared by addition of 30 mL of TEOS and 31 mL of Ethanol into a round-bottom flask and stirred under reflux. A mixture of distilled water (38 mL) and 0.1 mL of HCL was then added dropwise to the reaction mixture under constant stirring, resulting in a cloudy mixture. The solution was stirred until homogenous mixture was obtained before it was heated to $60°C$, followed by vigorous stirring for 4 h under reflux. The reaction mixture was then cooled to room temperature, followed by drying of the resulting silica sol in an oven at $60°C$ overnight. The collected silica sol was then crushed into fine particles, washed with distilled water to remove excess reactants, and subsequently dried in oven at $60°C$ for minimum of 12 h.

2.3. [EMIM][Tf₂N] Modified Silica Synthesis. Silica particles were modified via surface derivation method [31]. Known amount of synthesized silica particle was suspended in 100 mL of ethanol for 30 minutes and predetermined volume

IL:Si Ratio	Volume of IL (mL)	Mass of silica particles (g)
1.0:0.5	2.50	1.25
1.0:1.0	2.50	2.50
1.0:1.5	2.50	3.75
1.0:2.0	2.50	5.00
1.0:2.5	2.50	6.25

of $[EMIM][Tf_2N]$ was then added to the solution (Table 1). The reaction mixture was stirred at room temperature for 4 h. The sample was recovered via vacuum filtration and washed with distilled water before being dried in an oven at 60°C overnight. The investigated various IL:Si ratios are listed in Table 1. It is assumed that the surface derivation method is at concentration high enough to ensure the IL:Si ratio is significant between all samples.

2.4. Dense Flat Sheet Membrane Preparation. The dense flat sheet membrane was prepared from a solution consisting of PC (20 wt%), DCM (80 wt%), and modified silica particles (3 wt% of total polymer-solvent solution, optimum loading as recommended elsewhere [34]). The PC polymer was first dried in an oven at 60°C for 24 h to remove adsorbed moistures. The modified silica particles were dispersed into the DCM solvent and 20% of polymer was added under stirring for priming purpose. The mixture was stirred for 24 h at room temperature until the polymer granules were fully dissolved, followed by addition of remaining polymer. The mixture was further stirred for another 24 h. The homogeneous polymer solution was then degassed at room temperature using an ultrasonicator to remove any air bubbles formed during preparation. The polymer solution was then hand casted using a casting bar at a wet thickness of 100 μm. The casted film was then dried at room temperature for 24 h to ensure slow evaporation of the solvent. The pristine PC and PC-Sil membrane were prepared using the same process without the filler and pristine silica particles as filler, respectively.

2.5. Characterization. Fourier-Transform Infrared Spectroscopy (FTIR, Perkin Elmer Spectrum 1) was used to analyze the functional groups present in the modified silica particles. The powder sample and KBr were grounded before mixing. The powder was then added to a die-set to form a pellet before placed in the sample holder. The spectra were studied by coaddition of 20 scans in the range of 400-4000cm^{-1}. Within this range, the organic component converted the radiation into vibration.

X-ray Photoelectron Spectrometer (XPS, Thermo Scientific K-Alpha) analysis was used to determine the elemental composition of the synthesized modified silica particles. Chemical state analysis was done using XPS to analyze Si, H, O, F, N elements in the modified silica particles.

Differential Scanning Calorimeter (DSC, Q2000 TA) was used to determine the glass transition temperatures (T_g) of the fabricated MMM. The analysis was done at a temperature range of 50-250°C with a heating rate of 10°C/min. The sample was first heated in the first cycle to remove the thermal

history, then cooled at the same rate, and then heated again in the next heating cycle. The gas used in the analysis was nitrogen. The midpoint temperature of the transition region in the second heating cycle was determined as T_g.

Field Emission Scanning Electron Microscopy (FESEM, Zeiss Supra 55 VP) was used to characterize the surface morphology in the prepared MMMs. The MMMs were first fractured in liquid nitrogen, coated in gold/platinum, and placed in a sample holder before analysis. The thickness of the membranes was also determined from the FESEM images.

Gas permeation test was done by using a constant pressure variable volume method in a four channel permeation cells setup [34]. The membranes were tested against pure gases in a sequence from CH_4 to CO_2. The membranes were cut into 58 mm diameter circles using a circle cutter and were put into the permeation cells. The gas permeation test was done at pressures of 2 to 10 bar with incremental pressure of 2 bar at 24°C. A digital bubble flow meter (Humonics 420) was used to measure the permeate gas flow rates and the reading was repeated 3 times. The permeance, P/l (unit GPU), and permeability, P (unit barrer), are then evaluated using the following equation [34, 35]:

$$\frac{P}{l} = \frac{Q_{STP}}{A \cdot \Delta P} \tag{1}$$

$$P = \frac{Q_{STP} \cdot l}{A \cdot \Delta P} \tag{2}$$

where P/l represents the gas permeance (cm^3(STP)/(sec ·cm^2·cmHg)), Q_{STP} is the permeate flow rate at standard temperature and pressure in cm^3(STP)/sec, A is the effective membrane surface area (cm^2), and ΔP is the pressure gradient across the feed and permeate side of the membrane (cmHg). Gas permeance is usually reported in gas permeation unit GPU and Barrer, defined as

$$1 \; GPU = 10^{-6} \frac{cm^3 \, (STP)}{sec \cdot cm^2 \cdot cmHg} \tag{3}$$

$$1 \; Barrer = 10^{-10} \frac{cm^3 \, (STP) \cdot cm}{sec \cdot cm^2 \cdot cmHg} \tag{4}$$

The selectivity of the membranes, α, can then be evaluated as the ratio of the more permeable gas, i, to less permeable gas, j [34]:

$$\alpha_{i/j} = \frac{(P/l)_i}{(P/l)_j} = \frac{P_i}{P_j} \tag{5}$$

where $\alpha_{i/j}$ is the gas selectivity of gas penetrant i over gas penetrant j and P_i and P_j are the gas permeance of gas penetrant i and j, respectively.

3. Result and Discussion

3.1. Characterization of Modified Silica Particles. The FTIR spectra for virgin silica and the ionic liquid modified silica particles are presented in Figure 2. The FTIR spectra for virgin silica are in accordance with literature [31], confirming
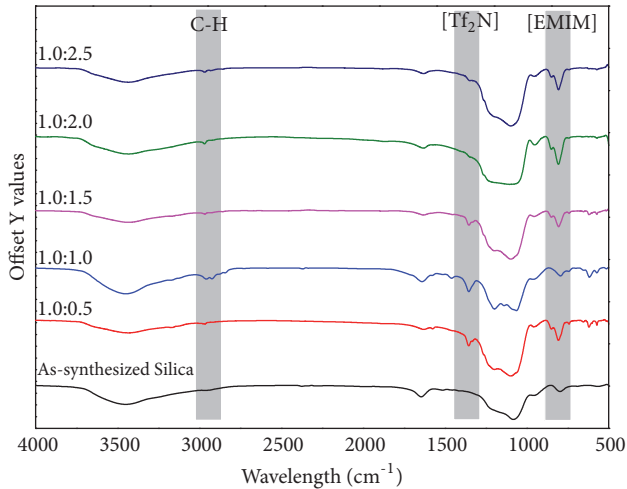
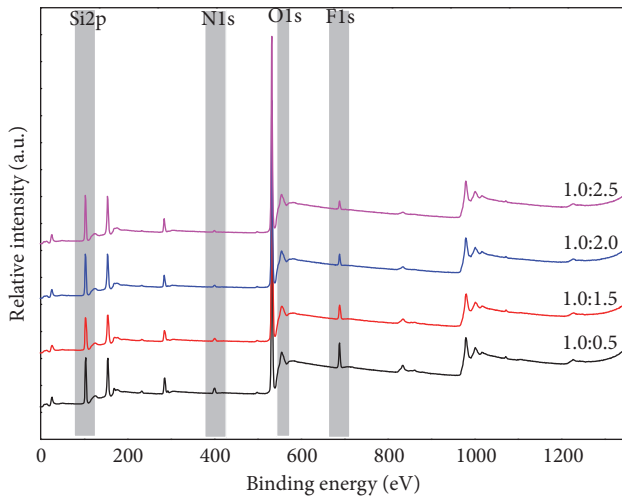Figure 2: FTIR spectra of virgin silica and ionic liquid modified silica particles.

Figure 3: XPS spectra of ionic liquid modified silica particles.

Table 2: Elemental composition of virgin silica and ionic liquid modified silica particles.

Sample	Element (wt%)			
	Si	N	O	F
Virgin Sil	39.39	-	60.61	-
1.0:0.5	50.58	2.21	42.29	4.92
1.0:1.0	49.87	0.32	49.24	0.57
1.0:1.5	51.71	1.46	43.46	3.48
1.0:2.0	53.26	1.00	43.64	2.10
1.0:2.5	54.14	0.61	43.75	1.50

Table 3: EDX elemental analysis of fabricated membranes.

Sample	EDX elemental analysis (wt %)			
	C	O	Si	F
PC-Sil	76.56	22.90	0.54	-
1.0:0.5	71.48	22.14	4.33	2.05
1.0:1.0	76.35	22.32	1.31	0.02
1.0:1.5	69.17	22.58	7.02	1.22
1.0:2.0	71.86	23.34	4.50	0.29
1.0:2.5	72.18	23.37	3.63	0.81

nitrogen elements in the modified particles, indicating a lower proportion of the IL presence. It should be noted that oxygen element decreased prominently after modification. This finding further suggests that the IL replaces the oxygen element onto the silica surface [31] and confirms the efficacy of the modification. As for 1.0:1.0 sample, the fluorine element is less than the other 4 samples. This shows that less fluorine was able to replace oxygen element onto the silica surface but still significant enough for the success of the surface derivation of silica. This result is also reflected on the shorter 734 cm^{-1} peak of 1.0:1.0 sample compared to other 4 modified silica sample further indicating the less amount of fluorine element.

3.2. MMM Characterization. The morphology of the fabricated membranes is presented in Figure 4, while their thicknesses are summarized in Table 4. In general, it can be observed that the membranes possess clear dense structure, especially for pure PC membrane (Figure 4(a)) and PC-Sil (Figure 4(b)). Interestingly, the presence of IL (from IL:Sil) causes the structure to has rougher cross-section (Figures 4(c)–4(g)), independent of the IL ratios. Since the filler loading was kept constant (3 wt% of total solids), this indicates the robust interface between PC matrix. Furthermore, lower amounts of silica fillers due to the presence of IL lead to rougher morphology compared to the pure PC and the PC-Sil membranes.

The EDX elemental scan result confirms the presence of the silica on all membranes observed based on the sharp peaks of silica (Table 3). Small amount of fluorine was also detected on all PC-Sil-IL MMMs as the IL contains fluorine. The amount of fluorine gradually decreases with increasing Si ratio accordingly. In addition, EDX mapping shows an even

the successful synthesis of the silica particles. Upon IL modification, the presence of additional broad bands, noticeably at 1354 cm^{-1} and 742 cm^{-1}, is observed. Both of the bands represent the characteristic bands of [EMIM][Tf$_2$N] which also show good agreement with literatures [31, 36]. Thus, these results confirm the successful attachment of the IL onto the surface of the silica particles. Increasing IL:Sil ratios however shows no observable changes on the obtained spectra.

Figure 3 shows the XPS spectra of IL-modified silica particles. The elemental compositions are summarized in Table 2. The as-synthesized silica particle is rich in Si and O, without presence of fluorine or nitrogen. The additional peaks of N1s (402.08eV) and F1s (688.68eV) are observed when IL is modified onto the silica particle, regardless of the IL ratio. These peaks further confirm chemical bonding of the ionic liquid onto the surface of the silica particles. The peak areas are determined and tabulated in Table 2 for each component. Increasing silica content decreases fluorine and
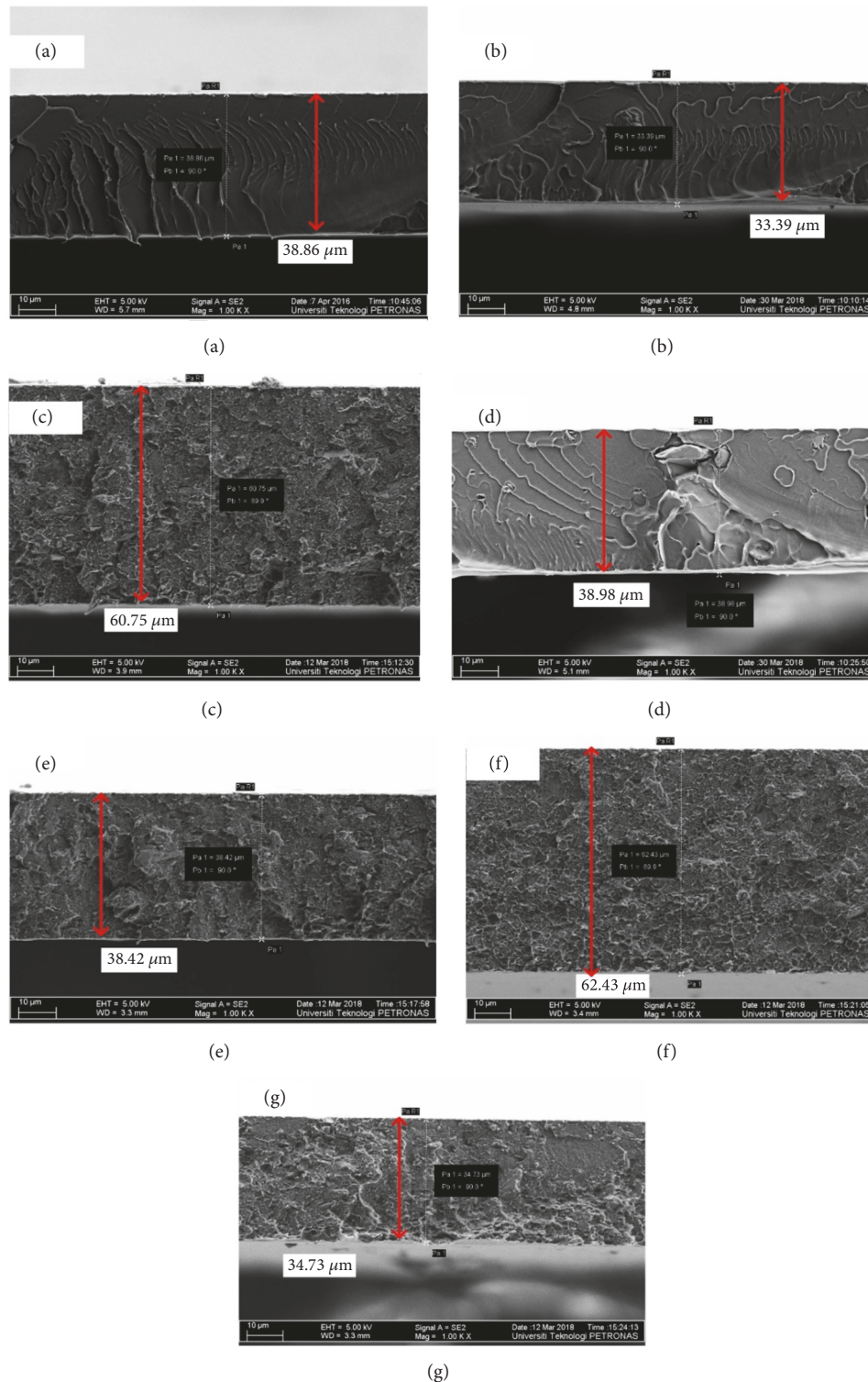
FIGURE 4: Cross-sectional membrane morphology of prepared membrane with (a) Pure PC, (b) PC-Sil, (c) 1.0:0.5, (d) 1.0:1.0, (e) 1.0:1.5, (f) 1.0:2.0, and (g) 1.0:2.5.

distribution of modified silica particles for all membranes (Figure 5).

The T_g of the prepared membranes are tabulated in Table 4. The T_gs of the pure PC and PC-Sil membrane are 143.38°C and 141.43°C, respectively, which are comparable with previous work [34]. The presence of IL lowers the T_g of the membrane which indicates the increase in polymer chain flexibility [37–41]. Since the filler loading was kept
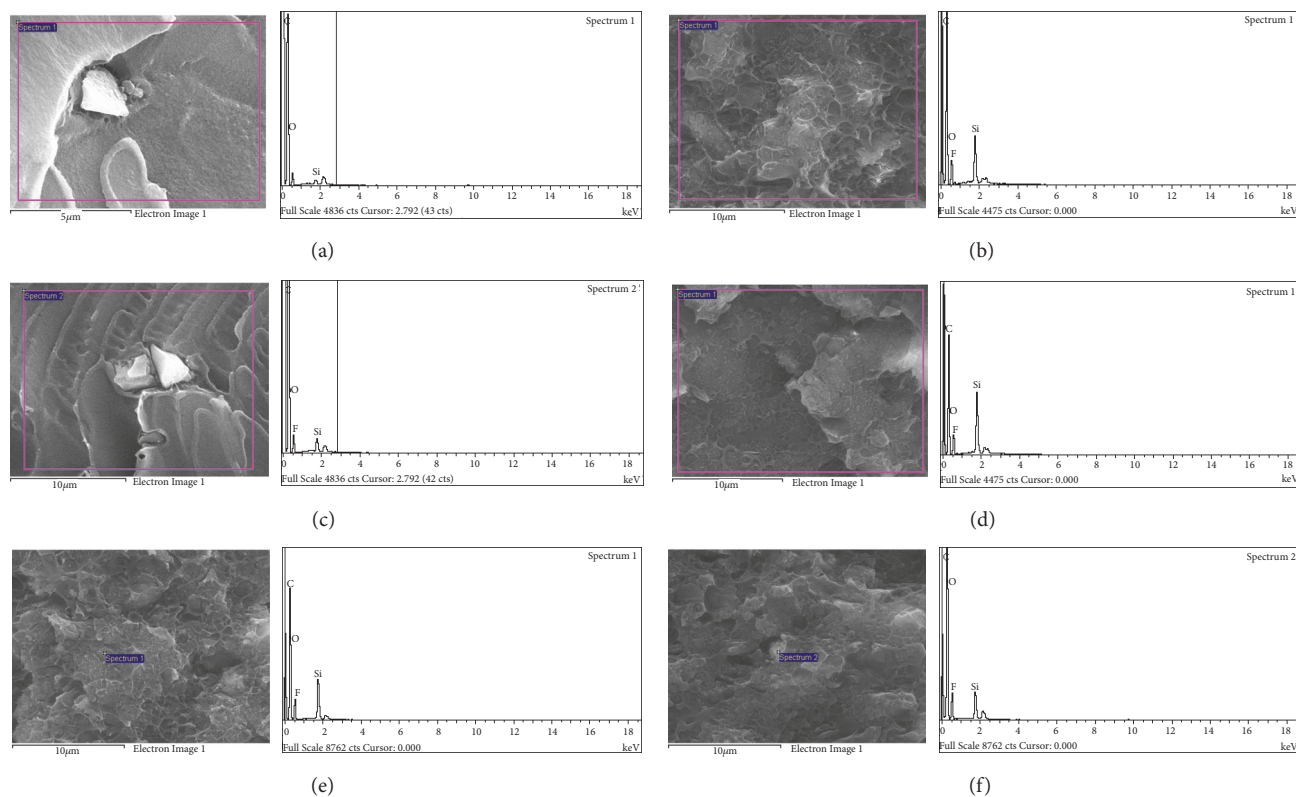
(a)

(b)

(c)

(d)

(e)

(f)

FIGURE 5: EDX spectra and electron images of prepared membranes with (a) PC-Sil, (b) 1.0:0.5, (c) 1.0:1.0, (d) 1.0:1.5, (e) 1.0:2.0, and (f) 1.0:2.5.

TABLE 4: Glass transition temperature (T_g) of prepared membranes.

Sample	Glass transition temperature (T_g)	Membrane thickness (μm)
Neat PC	143.38	38.86
PC-Sil	141.53	33.39
1.0:0.5	127.98	60.75
1.0:1.0	132.56	38.98
1.0:1.5	132.97	38.42
1.0:2.0	136.47	62.43
1.0:2.5	138.19	34.73

constant (3 wt% of total solids), this suggests that IL acts as a plasticizer, which reduces the overall rigidity and brittleness of the polymer chains, and softens the polymer matrix [38, 40, 41]. Estahbanati *et al.* [40] also highlighted that the addition of IL resulting in a more amorphous and less crystalline MMM.

3.3. Gas Permeation

3.3.1. Influence of Modified Silica on Membrane Performance. The fabricated pure PC membrane possesses CO_2 permeance of 13 GPU and CO_2/CH_4 selectivity of 18.5, comparable with other [34]. Upon incorporation of the synthesized silica (PC-Sil), a slight decrease in the CO_2 permeance to 7.57 GPU is observed while prominent increased in CO_2/CH_4 selectivity

to 25.96. The results can be attributed to the presence of silica within the MMM that contributes to higher solubilities and interactions of CO_2 with OH groups in silica particles [34, 42]. As a result, improvement in the selectivity with the expense of CO_2 permeance is observed.

Figure 6(a) shows the gas permeance of the PC-Sil-IL MMMs at feed pressure of 2 bar. Upon incorporating the IL-modified silica particles (PC-Sil-IL), both CO_2 permeance and CH_4 permeance increase prominently compared to the PC-Sil MMM. Remarkable improvements are shown for MMM with IL:Si ratio of 1.0:2.5, where the CO_2 and CH_4 permeance increase to 34.60 ± 0.26 GPU and 0.40 ± 0.001 GPU, respectively. The increase in gas permeance can be attributed to two main factors, namely, diffusivity and solubility. The presence of IL results in a more amorphous and flexible structure of MMM as observed by the T_g changes (Table 3), facilitating transport of gas molecules [37]. In addition, the relaxation of the polymer matrix and higher FFV with addition of IL also enhances gases diffusivity [38, 40]. The increment of diffusivity of gases is more prominent for gases with larger kinetic diameters, which explains the larger increase of diffusion for CH_4 than CO_2, which leads to an increase of permeability of CH_4 at higher IL loadings.

On the other hand, the increase of CO_2 permeability is also contributed by the increased solubility of CO_2 to the membrane through the presence of IL. The IL has high affinity towards CO_2; thus its presence leads to an increase of CO_2 solubility higher than CH_4 [36, 43]. The solubilities of CO_2 and CH_4 for [EMIM][Tf_2N] IL are 50 atm and
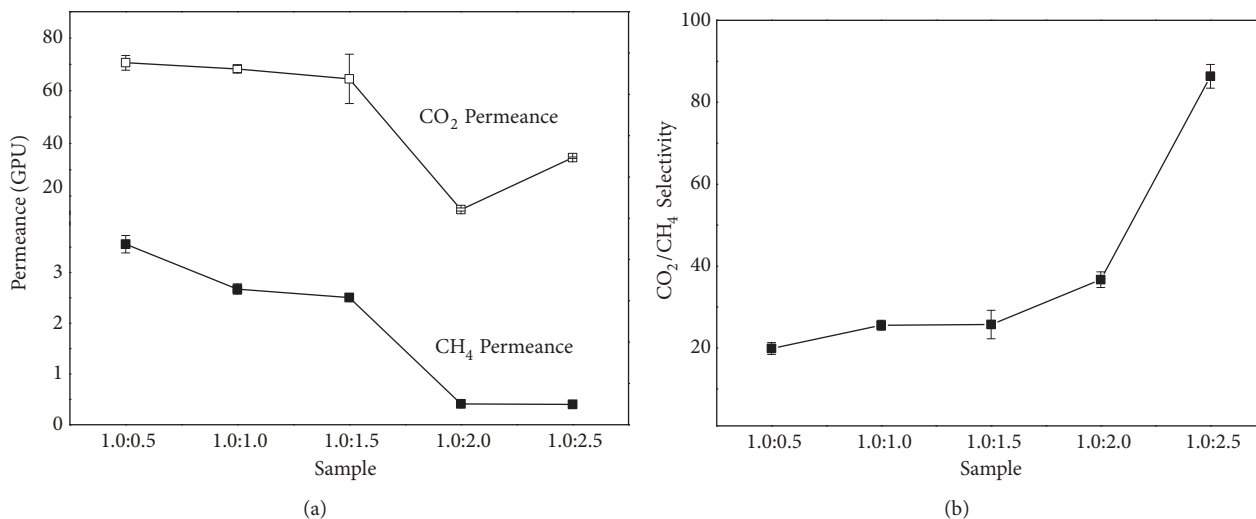
FIGURE 6: Separation performance of PC-Sil-IL at different IL:Si ratio at 2 bar with (a) gas permeance and (b) CO_2/CH_4 selectivity.

1200 atm in Henry constant at STP [36, 44]. The lower value of Henry's constant for CO_2 gas justifies the enhanced permeability of CO_2 due to the higher CO_2 solubility effect [36]. Similar trends have also been reported elsewhere [26, 28, 36, 38]. Thus, the combined effect of diffusivity and solubility increases gas permeance, in which CO_2 has more prominent increment than CH_4 owing to the presence of CO_2-philic IL.

The CO_2/CH_4 selectivity data of PC-Sil-IL membranes are shown in Figure 6(b). In general, the higher the IL content, the higher the CO_2/CH_4 selectivity due to the presence of higher CO_2-philic sites within the MMM. Interestingly, the highest IL content (sample IL:Si ratio of 1.0:0.5) shows the lowest selectivity of 19.90 ± 1.43, significantly lower than the PC-Sil MMM of 25.96. Only IL:Si ratio of 1.0:2.5 and 1.0:2.0 is superior to PC-Sil MMM. We propose that there are competition effects between solubility (from IL content) and diffusivity (from IL-induced plasticization). At high IL content (1.0:0.5), the CO_2 permeance increases by 832%, while CH_4 permeance increased by 11-fold as compared to PC-Sil. This indicates that the diffusivity factors induced by the IL-plasticization are superior thanks to the increased in the solubility, causing the more prominent increase in CH_4 permeance than CO_2. As the IL content is minimized, the effect of IL-induced plasticization is suppressed, as observed by increased in T_g (relative to 1.0:0.5). As a result, the IL-induce plasticization is less severe and the solubility factor becomes more dominant. Thus, the sample with lowest IL content (1.0:2.5) suppresses CH_4 permeance (decreased by 96%) while favors CO_2 to permeance (increased by 357%) relative to PC-Sil. The ideal selectivity of 1.0:2.5 is 85.10, which is 228% more superior to the PC-Sil.

3.3.2. Influence of Pressure on Membrane Performance.

Each prepared MMM was tested at different feed pressures to study the effect of pressure on its performance. The results are depicted in Figure 7. For all MMMs, both CO_2 permeance and CH_4 permeance show an overall decline with increasing pressure. This is in accordance with the dual-sorption model,

common for glassy polymers, such as PC. At low pressure, Henry and Langmuir sites are not saturated and the presence of microvoids allows for higher permeations [45, 46]. As pressure increases, the saturation of Henry and Langmuir sites would drastically reduce the pathway of permeation which then decreases the permeability of the MMM effectively. For all fabricated MMMs, there was no indication of plasticization phenomena as no obvious rise in permeance was observed at pressures up to 10 bar. This could be due to the fact that the strong ionic interactions from the IL could counteract the volume dilation induced by the absorbed CO_2.

All MMMs show an overall decreasing trend in selectivity with increasing pressure. This is due to the larger decrease in permeance of CO_2 gas compared to CH_4 gas from 2 bar to 10 bar, which affects the overall selectivity of the MMMs. This is justified by the saturation of sites at higher pressures affecting largely on the CO_2 permeability due to the higher solubility effect of CO_2 relative to CH_4 gas. Thus, increasing the concentration of the CO_2 penetrant would greatly reduce its permeability [34, 47]. Hassanajili *et al.* stated that, as hydrostatic pressure increases, the free volumes decrease, thus declining permeance and overall selectivity [47].

3.4. Comparison with 2008 Robeson Upper Bound.

The gas permeation performances of the fabricated MMMs are plotted on the Robeson's upper bound (Figure 8) by converting the permeation unit to barrer using (2) (the thickness of each membrane was based on the thickness observed via morphology (Table 4)). From the plot, it can be observed that all PC-Sil-IL MMMs at 2 bar performances fall in the attractive region, especially for PC-Sil-IL with IL:Si ratio of 1.0:2.5. Similar results also reported by Ban *et al.* [48] (CO_2 permeability of ~300 barrer and CO_2/CH_4 selectivity of 38) and Li *et al.* [30] (CO_2 permeability of ~100 barrer and CO_2/CH_4 selectivity of 36). The presence of $[EMIM^+Tf_2N^-]$ impregnated into their porous filler contributed to superior CO_2 permeability and CO_2/CH_4 selectivity, exceeding the
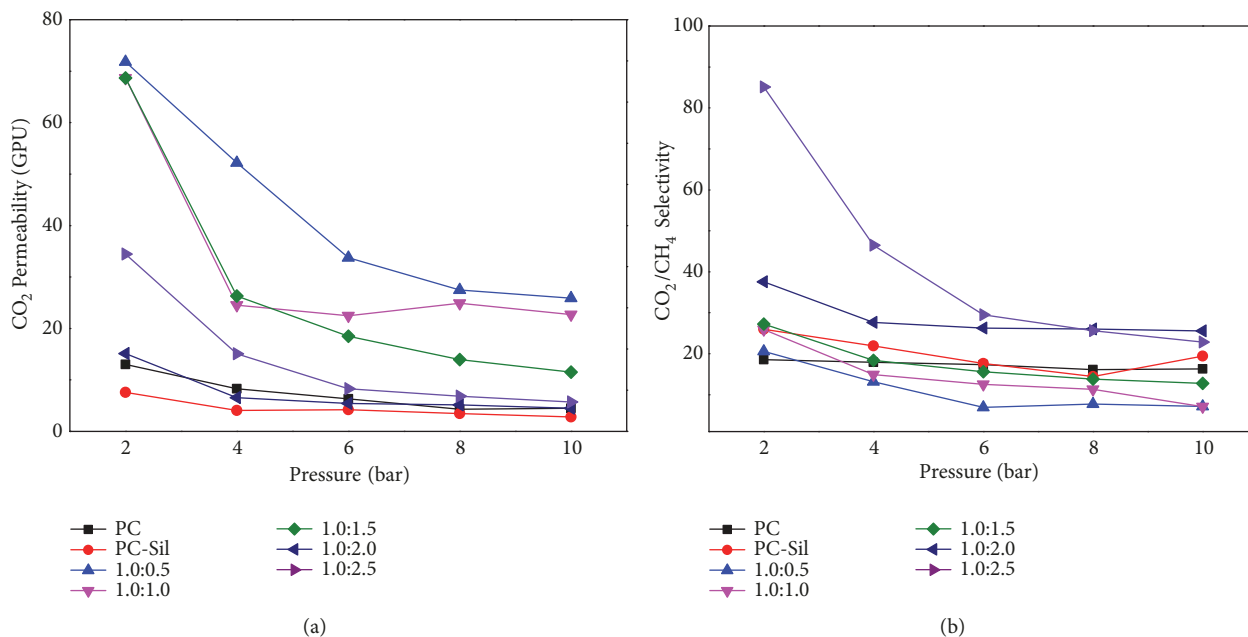
(a)

(b)

FIGURE 7: Effect of feed pressures on (a) CO_2 permeance, and (b) CO_2/CH_4 selectivity of prepared membranes.
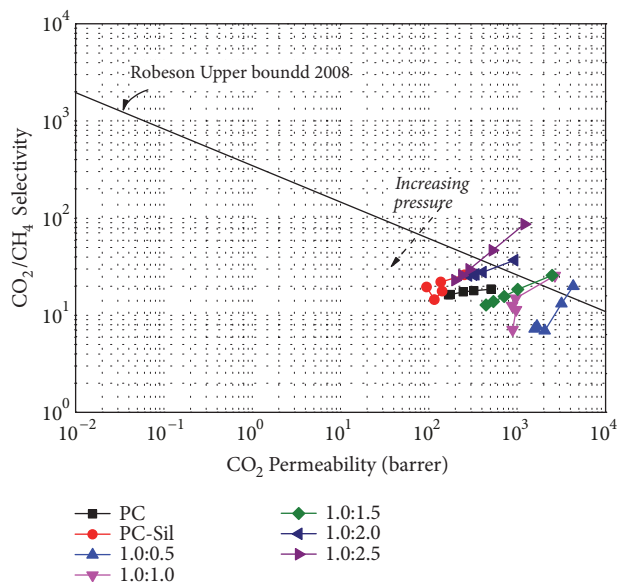

FIGURE 8: Comparison of membrane performance on 2008 Robeson's upper bound.

Robeson upper bound. However, with increasing pressure from 2 to 10 bar, the performance falls linearly towards below the line to the typical region, which obeys the dual-mode sorption theory, similar to that highlighted by previous researches [34, 47]. Overall results suggest that modification of silica particles with [EMIM$^+$Tf$_2$N$^-$] and embedding in PC matrix imparts superior gas separation properties at low pressure. However, further investigation of PC-Sil-IL should be conducted to study its performance at high pressures.

4. Conclusion

The effect of IL:Si ratio on the modified silica particles incorporated in PC polymer matrix was thoroughly investigated and discussed. The IL-modified silica has been successfully prepared as indicated from fluorine functional group from XPS and FTIR spectra. The presence of IL in the membrane resulted in rough morphology on the cross-section that is likely caused by the less robust interaction between PC and the fillers. Moreover, the ILs prompt higher polymer chain relaxation as observed in the decreased T_g. These results suggest that the presence of IL affects the resulting MMM properties, even at low concentrations. Gas permeation results show that increasing IL:Si ratio on the fillers reduces CO_2 permeability while increasing CO_2/CH_4 selectivity, with ratio of 1.0:2.5, gives the most promising results. The fabricated MMMs also show impressive capabilities of transcending the Robeson's upper bound at low pressure of 2 bar. An increment of 3-fold in CO_2/CH_4 selectivity was observed for the MMM with IL:Si ratio of 1.0:2.5 ratio. MMM with IL:Si of 1.0:2.5 ratio shows a desirable performance but further investigation with regard to the performance at high pressures should be considered.

Data Availability

The data used to support the findings of this study are included within the article.

Conflicts of Interest

The authors declare that there are no conflicts of interest regarding the publication of this paper.
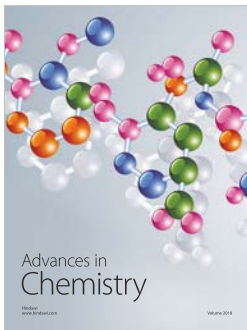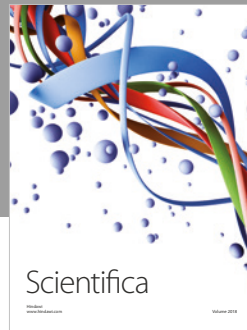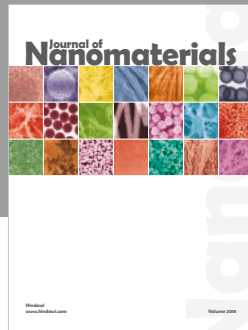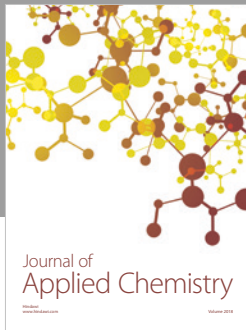
Acknowledgments

References

[1] K. M. Sabil, G.-J. Witkamp, and C. J. Peters, "Phase equilibria in ternary (carbon dioxide + tetrahydrofuran + water) system in hydrate-forming region: Effects of carbon dioxide concentration and the occurrence of pseudo-retrograde hydrate phenomenon," *The Journal of Chemical Thermodynamics*, vol. 42, no. 1, pp. 8–16, 2010.

[2] N. A. Md Nordin, S. M. Racha, T. Matsuura et al., "Facile modification of ZIF-8 mixed matrix membrane for CO2/CH4 separation: synthesis and preparation," *RSC Advances*, vol. 5, no. 54, pp. 43110–43120, 2015.

[3] Y. Zhang, J. Sunarso, S. Liu, and R. Wang, "Current status and development of membranes for CO2/CH4 separation: A review," *International Journal of Greenhouse Gas Control*, vol. 12, pp. 84–107, 2013.

[4] M. R. Othman, S. C. Tan, and S. Bhatia, "Separability of carbon dioxide from methane using MFI zeolite-silica film deposited on gamma-alumina support," *Microporous and Mesoporous Materials*, vol. 121, no. 1-3, pp. 138–144, 2009.

[5] Z. Y. Yeo, T. L. Chew, P. W. Zhu, A. R. Mohamed, and S.-P. Chai, "Conventional processes and membrane technology for carbon dioxide removal from natural gas: A review," *Journal of Natural Gas Chemistry*, vol. 21, no. 3, pp. 282–298, 2012.

[6] S. H. Han, J. E. Lee, K.-J. Lee, H. B. Park, and Y. M. Lee, "Highly gas permeable and microporous polybenzimidazole membrane by thermal rearrangement," *Journal of Membrane Science*, vol. 357, no. 1-2, pp. 143–151, 2010.

[7] N. Sazali, W. N. W. Salleh, N. A. H. Md Nordin, Z. Harun, and A. F. Ismail, "Matrimid-based carbon tubular membranes: The effect of the polymer composition," *Journal of Applied Polymer Science*, vol. 132, no. 33, 2015.

[8] R. W. Baker, *Membrane Technology and Applications*, McGraw-Hill, England, UK, 2004.

[9] L. M. Robeson, "The upper bound revisited," *Journal of Membrane Science*, vol. 320, no. 1-2, pp. 390–400, 2008.

[10] C. E. Powell and G. G. Qiao, "Polymeric CO2/N2 gas separation membranes for the capture of carbon dioxide from power plant flue gases," *Journal of Membrane Science*, vol. 279, no. 1-2, pp. 1–49, 2006.

[11] N. A. H. M. Nordin, A. F. Ismail, A. Mustafa, R. S. Murali, and T. Matsuura, "The impact of ZIF-8 particle size and heat treatment on CO2/CH4 separation using asymmetric mixed matrix membrane," *RSC Advances*, vol. 4, no. 94, pp. 52530–52541, 2014.

[12] N. A. H. M. Nordin, A. F. Ismail, A. Mustafa, R. Surya Murali, and T. Matsuura, "Utilizing low ZIF-8 loading for an asymmetric PSf/ZIF-8 mixed matrix membrane for CO2/CH4 separation," *RSC Advances*, vol. 5, no. 38, pp. 30206–30215, 2015.

[13] N. A. H. M. Nordin, A. F. Ismail, and N. Yahya, "Zeolitic imidazole framework 8 decorated graphene oxide (ZIF-8/GO) mixed matrix membrane (MMM) for CO2/CH4 separation," *Jurnal Teknologi*, vol. 79, no. 1-2, pp. 59–63, 2017.

[14] W. J. Koros, A. H. Chan, and D. R. Paul, "Sorption and transport of various gases in polycarbonate," *Journal of Membrane Science*, vol. 2, pp. 165–190, 1977.

[15] P. Hacarlioglu, L. Toppare, and L. Yilmaz, "Effect of preparation parameters on performance of dense homogeneous polycarbonate gas separation membranes," *Journal of Applied Polymer Science*, vol. 90, no. 3, pp. 776–785, 2003.

[16] P. Hacarlioglu, L. Toppare, and L. Yilmaz, "Polycarbonate-polypyrrole mixed matrix gas separation membranes," *Journal of Membrane Science*, vol. 225, no. 1-2, pp. 51–62, 2003.

[17] P. S. Goh, A. F. Ismail, S. M. Sanip, B. C. Ng, and M. Aziz, "Recent advances of inorganic fillers in mixed matrix membrane for gas separation," *Separation and Purification Technology*, vol. 81, no. 3, pp. 243–264, 2011.

[18] D. Gomes, S. P. Nunes, and K.-V. Peinemann, "Membranes for gas separation based on poly(1-trimethylsilyl-1-propyne)- silica nanocomposites," *Journal of Membrane Science*, vol. 246, no. 1, pp. 13–25, 2005.

[19] M. Vinoba, M. Bhagiyalakshmi, Y. Alqaheem, A. A. Alomair, A. Pérez, and M. S. Rana, "Recent progress of fillers in mixed matrix membranes for CO2 separation: A review," *Separation and Purification Technology*, vol. 188, pp. 431–450, 2017.

[20] J. Ahn, W.-J. Chung, I. Pinnau, and M. D. Guiver, "Polysulfone/silica nanoparticle mixed-matrix membranes for gas separation," *Journal of Membrane Science*, vol. 314, no. 1-2, pp. 123–133, 2008.

[21] R. Xing and W. S. W. Ho, "Crosslinked polyvinylalcohol-polysiloxane/fumed silica mixed matrix membranes containing amines for CO2/H2 separation," *Journal of Membrane Science*, vol. 367, no. 1-2, pp. 91–102, 2011.

[22] X. Y. Chen, Z. Razzaz, S. Kaliaguine, and D. Rodrigue, "Mixed matrix membranes based on silica nanoparticles and microcellular polymers for CO2/CH4 separation," *Journal of Cellular Plastics*, vol. 54, no. 2, pp. 309–331, 2018.

[23] Z. Lei, B. Chen, Y.-M. Koo, and D. R. Macfarlane, "Introduction: Ionic Liquids," *Chemical Reviews*, vol. 117, no. 10, pp. 6633–6635, 2017.

[24] J. Wang, "Recent development of ionic liquid membranes," *Green Energy & Environment*, vol. 1, no. 1, pp. 43–61, 2016.

[25] Z. Dai, R. D. Noble, D. L. Gin, X. Zhang, and L. Deng, "Combination of ionic liquids with membrane technology: A new approach for CO2 separation," *Journal of Membrane Science*, vol. 497, pp. 1–20, 2016.

[26] H. Z. Chen, P. Li, and T.-S. Chung, "PVDF/ionic liquid polymer blends with superior separation performance for removing CO 2 from hydrogen and flue gas," *International Journal of Hydrogen Energy*, vol. 37, no. 16, pp. 11796–11804, 2012.

[27] S. Uk Hong, D. Park, Y. Ko, and I. Baek, "Polymer-ionic liquid gels for enhanced gas transport," *Chemical Communications*, no. 46, pp. 7227–7229, 2009.

[28] L. Hao, P. Li, T. Yang, and T.-S. Chung, "Room temperature ionic liquid/ZIF-8 mixed-matrix membranes for natural gas sweetening and post-combustion CO2 capture," *Journal of Membrane Science*, vol. 436, pp. 221–231, 2013.

[29] Y. C. Hudiono, T. K. Carlisle, J. E. Bara, Y. Zhang, D. L. Gin, and R. D. Noble, "A three-component mixed-matrix membrane with enhanced CO2 separation properties based on zeolites and ionic liquid materials," *Journal of Membrane Science*, vol. 350, no. 1-2, pp. 117–123, 2010.

[30] H. Li, L. Tuo, K. Yang et al., "Simultaneous enhancement of mechanical properties and CO2 selectivity of ZIF-8 mixed

matrix membranes: Interfacial toughening effect of ionic liquid," *Journal of Membrane Science*, vol. 511, pp. 130–142, 2016.

[31] M. E. Mahmoud, "Surface loaded 1-methyl-3-ethylimidazolium bis(trifluoromethylsulfonyl)imide [EMIM+Tf2N-] hydrophobic ionic liquid on nano-silica sorbents for removal of lead from water samples," *Desalination*, vol. 266, no. 1-3, pp. 119–127, 2011.

[32] R. W. Baker and B. T. Low, "Gas separation membrane materials: a perspective," *Macromolecules*, vol. 47, no. 20, pp. 6999–7013, 2014.

[33] A. M. Buckley and M. Greenblatt, "The sol-gel preparation of silica gels," *Journal of Chemical Education*, vol. 71, no. 7, pp. 599–602, 1994.

[34] A. Idris, Z. Man, and A. S. Maulud, "Polycarbonate/silica nanocomposite membranes: Fabrication, characterization, and performance evaluation," *Journal of Applied Polymer Science*, vol. 134, no. 38, p. 45310-n/a, 2017.

[35] H. C. Koh, J. S. Park, M. A. Jeong et al., "Preparation and gas permeation properties of biodegradable polymer/layered silicate nanocomposite membranes," *Desalination*, vol. 233, no. 1-3, pp. 201–209, 2008.

[36] H. A. Mannan, H. Mukhtar, M. S. Shahrun, M. A. Bustam, Z. Man, and M. Z. A. Bakar, "Effect of [EMIM][Tf2N] Ionic Liquid on Ionic Liquid-polymeric Membrane (ILPM) for CO2/CH4 Separation," in *Proceedings of the 4th International Conference on Process Engineering and Advanced Materials, ICPEAM 2016*, pp. 25–29, Malaysia, August 2016.

[37] H. Rabiee, A. Ghadimi, and T. Mohammadi, "Gas transport properties of reverse-selective poly(ether-b-amide6)/[Emim][BF4] gel membranes for CO2/light gases separation," *Journal of Membrane Science*, vol. 476, pp. 286–302, 2015.

[38] D. F. Mohshim, H. Mukhtar, and Z. Man, "Composite blending of ionic liquid–poly(ether sulfone) polymeric membranes: Green materials with potential for carbon dioxide/methane separation," *Journal of Applied Polymer Science*, vol. 133, no. 39, 2016.

[39] Y. Qiu, J. Ren, D. Zhao, H. Li, and M. Deng, "Poly(amide-6-b-ethylene oxide)/[Bmim][Tf2N] blend membranes for carbon dioxide separation," *Journal of Energy Chemistry*, vol. 25, no. 1, pp. 122–130, 2016.

[40] E. Ghasemi Estahbanati, M. Omidkhah, and A. Ebadi Amooghin, "Preparation and characterization of novel Ionic liquid/ Pebax membranes for efficient CO2/light gases separation," *Journal of Industrial and Engineering Chemistry*, vol. 51, pp. 77–89, 2017.

[41] S. Kanehashi, M. Kishida, T. Kidesaki et al., "CO2 separation properties of a glassy aromatic polyimide composite membranes containing high-content 1-butyl-3-methylimidazolium bis(trifluoromethylsulfonyl)imide ionic liquid," *Journal of Membrane Science*, vol. 430, pp. 211–222, 2013.

[42] H. B. Park, J. K. Kim, S. Y. Nam, and Y. M. Lee, "Imide-siloxane block copolymer/silica hybrid membranes: Preparation, characterization and gas separation properties," *Journal of Membrane Science*, vol. 220, no. 1-2, pp. 59–73, 2003.

[43] S. Raeissi and C. J. Peters, "A potential ionic liquid for CO2-separating gas membranes: Selection and gas solubility studies," *Green Chemistry*, vol. 11, no. 2, pp. 185–192, 2009.

[44] A. Finotello, J. E. Bara, S. Narayan, D. Camper, and R. D. Noble, "Ideal gas solubilities and solubility selectivities in a binary mixture of room-temperature ionic liquids," *The Journal of Physical Chemistry B*, vol. 112, no. 8, pp. 2335–2339, 2008.

[45] E. S. Sanders, "Penetrant-induced plasticization and gas permeation in glassy polymers," *Journal of Membrane Science*, vol. 37, no. 1, pp. 63–80, 1988.

[46] S. Subramanian, J. C. Heydweiller, and S. A. Stern, "Dual-mode sorption kinetics of gases in glassy polymers," *Journal of Polymer Science Part B: Polymer Physics*, vol. 27, no. 6, pp. 1209–1220, 1989.

[47] S. Hassanajili, M. Khademi, and P. Keshavarz, "Influence of various types of silica nanoparticles on permeation properties of polyurethane/silica mixed matrix membranes," *Journal of Membrane Science*, vol. 453, pp. 369–383, 2014.

[48] Y. Ban, Z. Li, Y. Li et al., "Confinement of Ionic Liquids in Nanocages: Tailoring the Molecular Sieving Properties of ZIF-8 for Membrane-Based CO2 Capture," *Angewandte Chemie International Edition*, vol. 54, no. 51, pp. 15483–15487, 2015.

The Scientific World Journal

Journal of Applied Chemistry

Journal of Nanomaterials

Scientifica

International Journal of Polymer Science

Advances in Chemistry

Advances in Physical Chemistry

International Journal of Analytical Chemistry
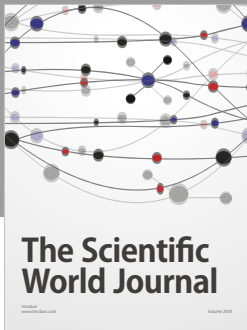
Hindawi

Submit your manuscripts at

www.hindawi.com

Advances in Condensed Matter Physics

Journal of Chemistry

International Journal of Biomaterials

Advances in High Energy Physics

Journal of Engineering

Journal of Nanotechnology

International Journal of Corrosion

Journal of Materials

BioMed Research International

Advances in Tribology

Advances in Materials Science and Engineering